Hindawi Publishing Corporation
International Journal of Photoenergy
Volume 2008, Article ID 524142, 7 pages
doi:10.1155/2008/524142

Research Article

Light-Induced Tyrosine Radical Formation from Ruthenium-Tyrosine Complex Anchored to SnO_2 Semiconductor

Raed Ghanem

Department of Chemistry, University of Al al-Bayt, P.O. Box 130040, Mafraq 25113, Jordan

Correspondence should be addressed to Raed Ghanem, raedsa@yahoo.com

Received 4 August 2007; Revised 26 October 2007; Accepted 10 December 2007

Recommended by Panagiotis Lianos

Steady state spectroscopy and flash photolysis measurements were used to study the multistep electron transfer in a supramolecular complex adsorbed on the surface of nanocrystalline SnO_2 in order to mimic the function of the tyrosine$_Z$ and chlorophyll unit P_{680} in natural photosystem II (PSII). A ruthenium(II)-tris(bipyridyl) complex covalently linked to an *L*-tyrosine ethyl ester through an amide bond was anchored to the surface of nanocrystalline SnO_2 via four carboxylic acid groups linked to the bpy ligands. The apparent association constant for the association between ruthenium(II)-tris(bipyridyl) complex and SnO_2 is $3.2 \times 10^6\ M^{-1}$ and a degree of association up to 99% was determined. 450 nm excitation of the complex promotes an electron to a metal-to-ligand charge transfer (MLCT) excited state, from which the electron is injected into SnO_2. The photogeneration of Ru(III) is followed by an intramolecular electron transfer from tyrosine to Ru(III), regenerating the photosensitizer Ru(II) and forming the tyrosyl radical. The tyrosyl radical is formed in less than 3 microseconds with a yield of 32%.

1. INTRODUCTION

Production of tyrosine radical (Tyr_Z) is the primary step on the photosynthetic energy conversion in plants due to the crucial role of the Tyr_Z in photosynthetic energy conversion through the oxidation of water into molecular oxygen. This process (regardless of the exact mechanism of photosynthetic water oxidation) [1–5] is initiated when the primary donor chlorophyll P_{680} absorbs light, which results in transferring an electron from the excited state chlorophyll, via several steps, to quinone on the acceptor side of PSII, leading to the oxidation of P_{680}, in which P_{680}^+ is produced. Moreover, photogenerated P_{680}^+ recaptures an electron by oxidizing a nearby tyrosine (Tyr_Z) into a neutral tyrosyl radical ($Tyr_Z^\bullet$) [3, 4]. Once the tyrosyl radical is formed, it oxidizes the water molecule by one of two mechanisms. (I) The radical in its turn oxidizes a tetranuclear Mn-cluster bound to PSII, and after four consecutive turnovers, two water molecules are oxidized into molecular oxygen; (II) tyrosine radical (Tyr_Z) catalyzes water oxidation by abstracting a hydrogen atom from a water molecule coordinated to the manganese cluster Mn_4 [1, 2].

Efforts to design supramolecular complexes to mimic the important part of light-driven process in PSII in order to construct an artificial photosynthetic system for fuel production are continuous. Ruthenium-tris(bipyridine) complexes have been used as a model compound to mimic the PSII photochemistry in which ruthenium acts as a photosensitizer in analogy of P_{680} in PSII. In previous studies, model complexes (Ru(II)(bpy(COOH)$_2$)$_2$(4-Me-4′CONH$_{\text{-L-}}$-tyrosine ethyl ester-2,2′-bpy) $2PF_6$ (**1**) with its analogue (**1a**) and (Ru(II)(bpy)$_2$(4-Me-4′-CONH$_{\text{-L-}}$-tyrosine ethyl ester-2,2′-bpy)) $2PF_6$ (**2**) were studied to mimic the Tyr_Z-P_{680} functional unit of PSII by generating a tyrosyl radical by means of intramolecular electron transfer from the tyrosine moiety to the photogenerated Ru(III) (i.e., upon excitation of Ru(II)(byp)$_3$ moiety with visible light, electrons are transferred from the excited state of the Ru(II) to an electron acceptor producing Ru(III), then an electron is transferred to the oxidized ruthenium from tyrosine moiety leading to recovery of Ru(II) and tyrosyl radical formation [6–9]). Also it was found that in the presence of an external electron acceptor (i.e., methyl viologen or cobalt pentaaminechloride), the photogenerated tyrosyl radical can

oxidize a binuclear manganese cluster from its Mn(III/III) state to the Mn(III/IV) state [8, 9]. Despite the proven functionality of the artificial system, the use of an external electron acceptor has the disadvantage of diffusion-limited electron transfer from the excited state of the ruthenium complex to the external electron acceptor [6–9]. However, it was demonstrated that the use of a nanocrystalline semiconductor (i.e., TiO_2) as an electron acceptor with Ru-tyrosine complex overcomes the diffusion-controlled nature of the electron transfer since the electron injection was reported to occur on femtosecond to picosecond time scale [10]. Also, the possibility of multistep electron transfer in complex (**1**) adsorbed on the surface of TiO_2 via four carboxylic acid groups linked to the bpy ligands was demonstrated. Excitation of complex (**1**) promotes an electron to a metal-to-ligand charge transfer (MLCT) excited state from which the electron is injected into TiO_2 resulting in the formation of Ru(III). The photogeneration of Ru(III) is followed by an intramolecular electron transfer from tyrosine to Ru(III) regenerating the photosensitizer Ru(II) and forming the tyrosyl radical with a yield of 15%. The low yield of tyrosine production is a result of a fast back electron transfer reaction from the nanocrystalline TiO_2 to the photogenerated Ru(III) [10]. Most of ultrafast interfacial electron transfer studies are focused on TiO_2 where the rate of electron injection of dye adsorbed onto TiO_2 was reported to be multiexponential and mainly in the femtosecond regime [11–14]. Recently, it was demonstrated that other wide bandgap semiconductors like SnO_2 and ZnO are promising [15]. In this paper, we will demonstrate the possibility of obtaining a multistep electron transfer in a supramolecular complex (**1**) anchored to nanocrystalline Tin(IV) dioxide (SnO_2) with a target to improve the efficiency of tyrosine radical production (see Figure 1).

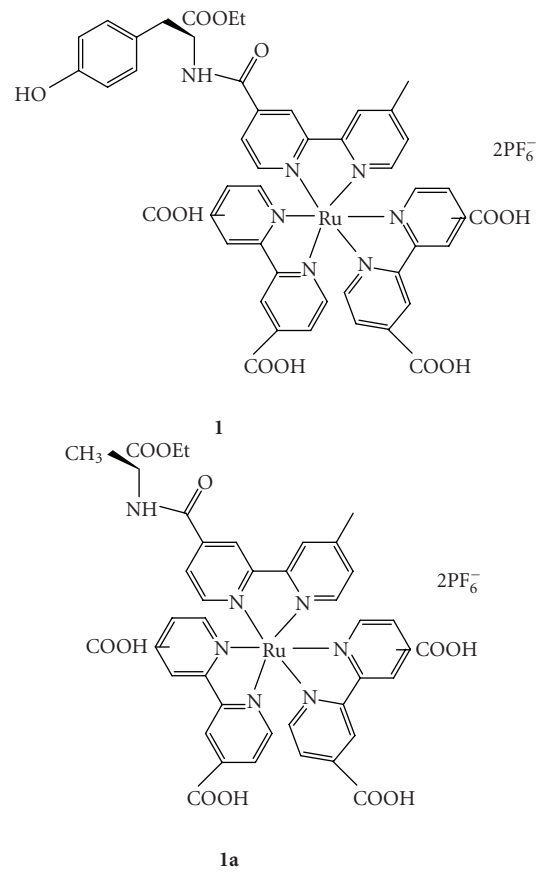

Figure 1: Chemical structure of complexes (**1**) and (**1a**).

2. EXPERIMENTAL SECTION

2.1. Materials

Synthesis and characterization of Ru-(II)(bpy(COOH)$_2$)$_2$(4-Me-4′CONH$_{-L-}$tyrosine ethyl ester-2,2′-bpy) $2PF_6$ (**1**) and its analogue Ru(II)-tris(bipyridyl) (**1a**) have been described elsewhere [10]. A stable suspension (15%) of SnO_2 was purchased directly from Alfa Chemicals.

The stock solutions of (**1**) and (**1a**) were prepared in methanol and stored in the dark. The sample solutions were prepared in water by adding a few microliters of SnO_2 solution to freshly prepared solutions of (**1**) or (**1a**) to obtain the desired concentration. Sample degradation was checked out by measuring the absorption spectra before and after flash photolysis measurements—no sample degradation was observed during the flash photolysis experiment. The pH of the solution was adjusted with HCl or NaOH and measured with a Metrohm pH meter.

2.2. Spectroscopic measurements

Luminescence spectra were recorded using a SPEX Fluorolog fluorimeter by exciting the sample at 450 nm. Absorption spectra were recorded on a Jasco-V-530 spectrophotometer in a 1 cm quartz cell. Transient absorption experiments were conducted with a nanosecond laser flash photolysis setup. The excitation pulse at 450 nm was obtained from a Quanta-Ray master optical parametric oscillator (MOPO) pumped by a Quanta-Ray 230 Nd:YAG laser, having a pulse energy of 1-2 mJ and duration of approximately 7 nanoseconds. The probe light from a xenon arc lamp (75 W) was focused to a 1 mm diameter spot overlapping with the unfocused pump beam of 2.5 mm diameter. After the 1 cm quartz cell containing the sample, the probe light was passed through two single grating monochromators and detected by a photomultiplier tube (Hamamatsu R928).

The transient spectra at different delay times were constructed from average kinetic traces measured at different wavelengths. All kinetic traces and spectral profiles were fitted using the data-analysis package Microcal Origin.

3. RESULTS AND DISCUSSION

The absorption and emission spectra of (**1**) and (**1a**) (Figure 2) were similar to those of $Ru(bpy)_3^{+}$ complexes [16, 17]; the intense band at ~300 nm is attributed to the ligand-centered (LC) band which arises from a π to π^* transition.

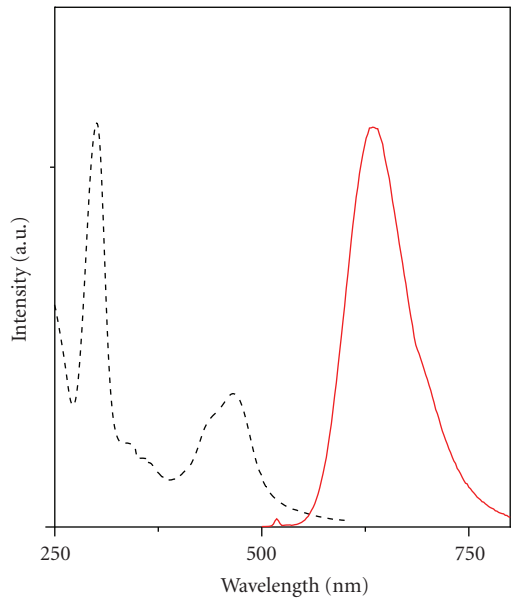

Figure 2: Normalized absorption and emission spectra of complex (**1**). The emission spectra were excited at 450 nm.

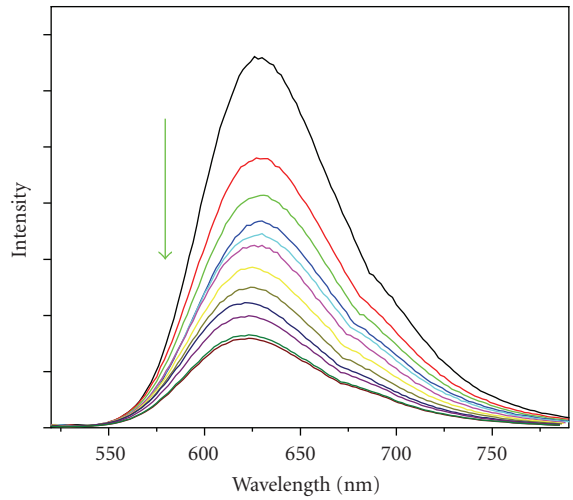

Figure 3: Luminescence emission spectra of complex (**1**) in the presence of various concentrations of SnO_2.

The band at 475 nm which was assigned to a metal-to-ligand charge transfer (MLCT) as a result of a d to π^* transition is red-shifted by ~25 nm (depending on the pH) compared to $Ru(bpy)_3^{+}$ complexes [16, 17] due to the carboxylate substituents. Deprotonation of the carboxylic acid group affects the LUMO energy of the ligand. The MLCT band is blue-shifted to higher energy by 10 nm upon increasing the pH of the solution from 1 to 7 [18, 19]. The shift of the MLCT absorption band at 470 nm of (**1**), as a function of pH, was used to determine the pK_a value of the ground state [20]. The analysis of the pH profile of (**1**) resulted in two inflection points at pH = 0.4 and pH = 2 which were attributed to the loss of two carboxylate protons at each inflection point.

The emission intensity also shows a pH dependence; the lowest MLCT excited state exhibits an intense luminescence emission band at ~625 nm, at pH 7, and it is red-shifted by ~25 nm at pH 1 (~650 nm). The pH dependence can be explained by the differences in electron accepting/donating properties of the protonated/deprotonated forms of the ligands [10].

SnO_2 has an isoelectric point at pH ~3.5 [15]; that is, at pH < 3.5, SnO_2 is positively charged [$SnOH^+$]; thus, a condition of pH < 3.5 represents an optimal condition for the electrostatic attraction for the adsorption of (**1**) and (**1a**) onto the surface of the semiconductor (i.e., pK_a values of (**1**) are 2 and 0.4). The quenching of the emission spectra of complexes (**1**) and (**1a**) with the addition of SnO_2 was used to study the efficiency of the attachment of both complexes (**1**) and (**1a**) onto the surface of the SnO_2. The luminescence intensity of (**1**) is decreased with the increase of SnO_2 concentration until it reaches a constant value at 90 μM [SnO_2] (see Figure 3). Moreover, the adsorption of (**1**) onto the surface of SnO_2 causes a small blue shift (from 430 nm to 420 nm); in fact, this observation is completely opposite to the previously reported system of 1-TiO_2 where a red shift was observed and attributed for the delocalization of π^* orbital [10] of the bipyridine ring with conduction band. The origin of the blue shift observed for 1-SnO_2 could be attributed to (I) aggregation behavior of (**1**) on the surface of SnO_2, (II) fully deprotonation of (**1**), and (III) a weak electronic coupling between the dye molecule and the semiconductor surface. In fact, similar blue shift has been reported for other ruthenium dye, N719, adsorbed onto the surface of nanocrystalline SnO_2 [15], and it is also observed for other molecular dyes such as perylene adsorbed onto nanocrystalline SnO_2 [21]. On the other hand, the similarity of the quenching pattern observed for both complexes shows that the presence of tyrosine in (**1**) does not affect the functionality of the carboxylic acid group; therefore, the steady state analysis is valid for (**1**) and (**1a**).

The observed quenching of the MLCT was attributed to an electron injection from the excited state of the dye into the conduction band of SnO_2 [13, 22–26]. Energy differences between the conduction band of the semiconductor and the redox potential of the excited ruthenium, $E_{Ru^{(III/II)}}$, are the major driving forces for the electron injection. It is not possible to electrochemically determine the $Ru^{(III/II)}$ oxidation potential in aqueous media because of the background water oxidation current; however, the $Ru^{(III/II)}$ redox potential could be estimated from the value of $Ru(dcb)_3^{2+}$ in acetonitrile [27, 28]; the $Ru^{(III/II)}$ redox potential is estimated versus NHE electrode to be 1.37 eV and 1.2 eV for the fully protonated and deprotonated forms of complex (**1**), respectively. Taking into account the excited state energy of (**1**) (c.a 2 eV, λ_{max} ~470 nm) and the energy band-gap of SnO_2 (approximately 3.8 eV), we can conclude that the electron injection from the excited state of the dye into the conduction band of semiconductor is thermodynamically allowed. Kamat [23] relates the quenching of the excited state by colloidal semiconductor to the adsorption of the dye onto the surface of semiconductor (i.e., SnO_2). The extent of the quenching of fluorescence intensity by the SnO_2 colloidal particle reflects

the amount of chemisorbed dye onto the surface of the SnO_2 particle. In order to obtain an association constant (K_a) for the dye-SnO_2 interaction, quenching of the luminescence intensity of (**1**) and (**1a**) by SnO_2 was analyzed by considering an equilibrium between the adsorbed and unadsorbed dye molecules:

$$\text{Dye–COO}^- + \text{SnOH}^+ \overset{K_a}{leftarrows} [\text{Dye–COO–Sn} \equiv]. \quad (1)$$

The observed emission quantum yield ϕ_f of the dye in the presence of colloid is related to the emission quantum yield of the unadsorbed dye ϕ_f^o and the emission quantum yield of the adsorbed molecule, ϕ_f', as follows:

$$\phi_f = (1-\alpha)\phi_f^o + \alpha\phi_f', \quad (2)$$

where α is the degree of association between the SnO_2 particles and complex (**1**). Under pseudo-first-order reaction condition ($[SnO_2] \gg [\text{dye}]$), α can be expressed as

$$\alpha = \frac{K_a[SnO_2]}{1 + K_a[SnO_2]}. \quad (3)$$

By substituting (3) into (2), the quenching of luminescence emission of (**1**) or (**1a**) by SnO_2 can be represented as

$$\frac{1}{(\phi_f^o - \phi_f)} = \frac{1}{(\phi_f^o - \phi_f')} + \frac{1}{K_a(\phi_f^o - \phi_f')[SnO_2]}. \quad (4)$$

The emission quantum yields (ϕ) were measured by comparison of the emission spectrum of the sample with the emission spectrum of a reference compound (tryptophan) using the following equation:

$$\phi_x = \frac{D_x}{D_r}\frac{A_r(\lambda_r)}{A_x(\lambda_x)}\phi_r, \quad (5)$$

where D is the area under the luminescence spectrum, $A(\lambda)$ is the corresponding absorbance at the excitation wavelength, and the subscripts r and x refer to reference and sample solutions [24]. Plot of the emission quantum yield of the dye complex (**1**) in the presence of SnO_2 colloidal versus the concentration of SnO_2 according to (4) results in straight line (linear fitting results with correlation coefficient R of 0.998) in which the apparent association constant and the emission quantum yield of the adsorbed molecule could be estimated from the slope and intercept, respectively. The apparent association constant of $2.3 \times 10^6\ \text{M}^{-1}$ and the emission quantum yield of the adsorbed molecule ($\phi_f' \sim 0.002$) were obtained with a degree of association equal to 99% (i.e., 99% of complex (**1**) adsorbed onto the surface of SnO_2). Again, a similar pattern was observed for the reference compound (**1a**).

Figure 4 shows the transient absorption spectra of complexes (**1**) and (**1a**) (20 μM of (**1**)/(**1a**) and 90 μM of SnO_2 at pH ~ 2). The photoinduced electron transfer processes were initiated with the excitation of MLCT (through absorption of photon at $\lambda = 450$ nm) which promotes the electron from a Ru d-orbital to π^* orbital of the ligand, from which an electron can be injected into the conduction band of SnO_2. The above mechanism leads to the formation of Ru(III) cation and the bleaching of Ru(II) MLCT ground state [18, 26]. Analogously to other ruthenium complexes and taking into account the energetic point of view, we can assume that the electron transfer from the dye to SnO_2 occurs in an ultrafast subpicosecond to femtosecond time scale [15, 22]. For ruthenium-tyrosine complexes (like complex (**1**)) anchored to the nanocrystalline semiconductors, the second electron transfer from the tyrosine moiety to the dye cation Ru(III) is the rate-limiting step. The photogenerated Ru(III) can return to the Ru(II) ground state either by charge recombination (back electron transfer from the nanocrystalline SnO_2) or by a second intramolecular electron transfer process from the linked tyrosine moiety [7, 9]. Distinguishing between these two ways needs a careful investigation of the transient absorption spectra.

The time evolution of the transient absorption spectra of the (**1**)-SnO_2 system, Figure 4(a), shows that the absorption recovery of Ru(II) is accompanied by the formation of a tyrosyl radical which is known to have an absorption band at 410 nm (i.e., the positive signal at 410 nm) [29]. Tyrosyl radical is indeed formed as a result of the intramolecular electron transfer from the tyrosine moiety to the photogenerated Ru(III). The confirmation of the above conclusion was achieved in a separate experiment on the analogue complex (**1a**) which lacks the tyrosine moiety; therefore, no absorbance feature due to the generation of tyrosyl radical should be observed [10]. The transient absorption spectra of complex (**1a**) anchored to SnO_2. Figure 4(b) shows that the strong bleaching of the MLCT band (as a result of the electron injection into the SnO_2) was followed by an absorption recovery at 470 nm (as a result of recombination between electrons in the nanocrystalline SnO_2 and Ru(III)). As it was previously illustrated for (**1**) or (**1a**)-TiO_2 systems, the absorption recovery of the reference complex (**1a**) is apparently slower than the absorption recovery recorded for complex (**1**) (the bleaching signal of complex (**1**) is completely recovered within, approximately, 80 microseconds, whereas it was not recover for complex (**1a**)); in fact, the recovery of the bleaching signal in the (**1**)-SnO_2 system is indeed faster than the (**1**)-TiO_2 system.

The yield of Ru(III) to tyrosyl radical can be estimated from the relative absorption magnitude of Ru(II) ground state bleaching at early times and from the 410 nm band corresponding to the tyrosyl radical; the absorption coefficient of the tyrosyl radical is $\varepsilon = 3000\ \text{M}^{-1}\text{cm}^{-1}$, and for complex (**1**) it is $\varepsilon = 15000\ \text{M}^{-1}\text{cm}^{-1}$. Despite the fact that the electron injection rate for the Ru-SnO_2 system is slower than the Ru-TiO_2 system [10], it is interesting to observe that for (**1**)-SnO_2 system the yield of Ru(III) to tyrosyl radical conversion was about 32% compared to 15% for (**1**)-TiO_2 system. The relatively low yield of tyrosine-Ru(III) electron transfer into TiO_2 was explained by a fast back electron recombination process from TiO_2 to Ru(III). Indeed, in the case of electron transfer from Ru(III) to SnO_2, the charge recombination seems to be slower than the case of TiO_2 (recombination rate constants are $8.0 \times 10^4\ \text{s}^{-1}$ and $1.1 \times 10^5\ \text{s}^{-1}$ for (**1**)-SnO_2 and (**1**)-TiO_2 systems, resp.) which could be attributed to the efficiency of attachment of complex (**1**)

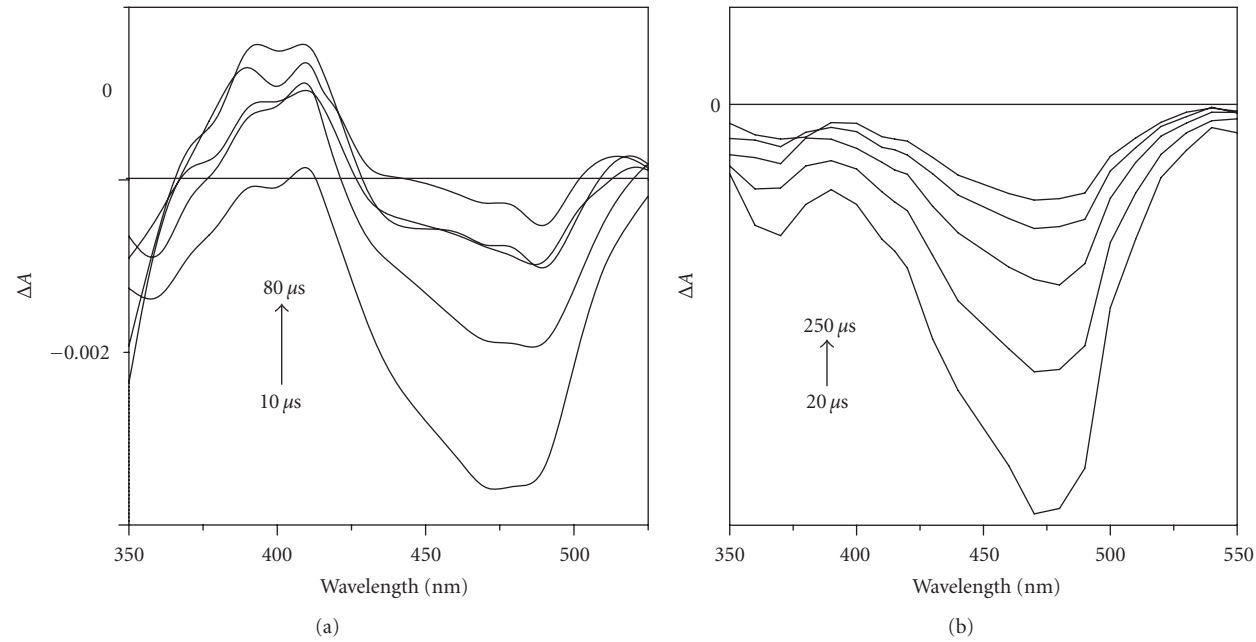

Figure 4: Transient absorption spectra of adsorbed complexes (**1**) (a) and (**1a**) (b) at pH 2 with 90 μM of SnO_2 at different delay times after excitation at 450 nm.

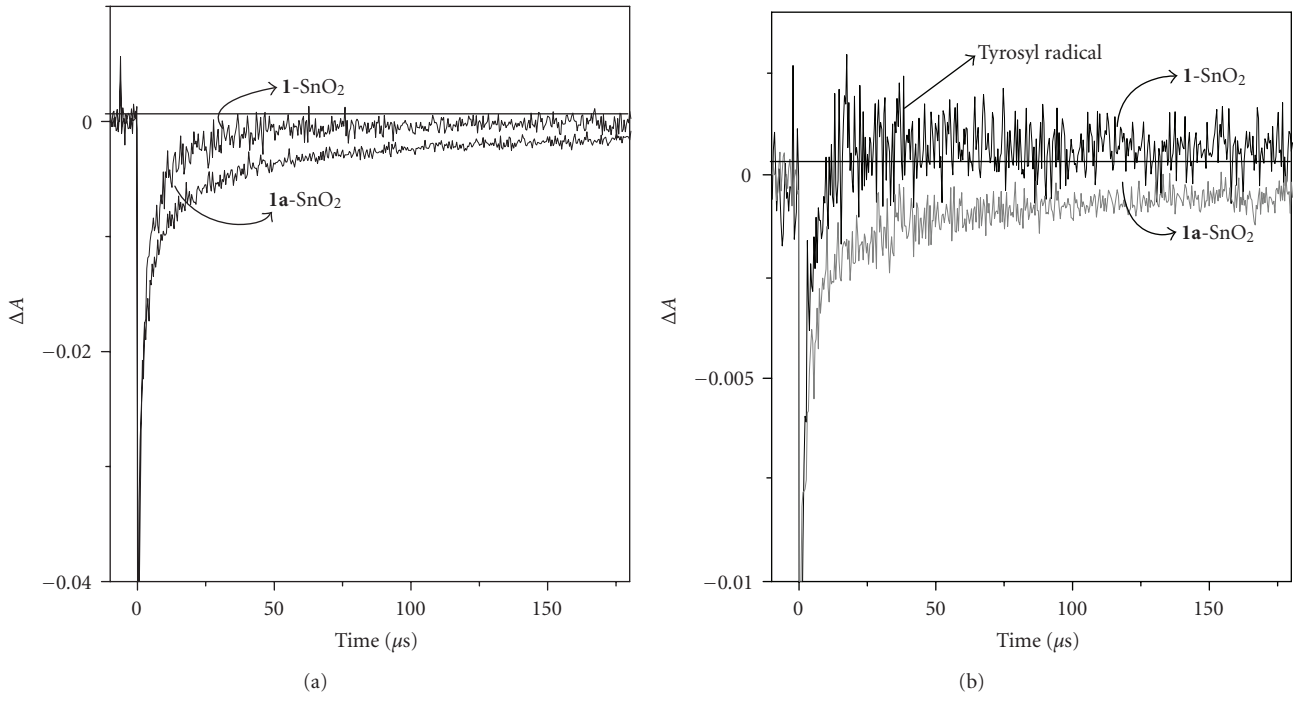

Figure 5: Kinetics of the adsorbed complexes (**1**) and (**1a**) measured after 450 nm excitation at pH 2 with 90 μM of SnO_2; the kinetics were recorded at 470 nm (a) and at 410 nm (b).

onto the surface of SnO_2 (~99% adsorption); the above analysis was confirmed through the comparison of the kinetics of Ru(II) absorption recovery at 470 nm for complexes (**1**) and (**1a**) (Figure 5). The absorption recovery of complex (**1a**) reflects only the dynamic of the charge recombination of (**1a**) and SnO_2 since it was the only pathway of the recovery of the excited Ru(II); thus, a direct comparison of the kinetics shown in Figure 5 enables us to obtain the time constants of tyrosine-Ru(III) electron transfer and the back electron transfer recombination. A multiexponential fit of the kinetics data for complex (**1a**) at 470 nm results in time constants of $\tau_1 \approx 0.5$ (60%) microsecond and

$\tau_2 = 30.6 \pm 0.5$ (40%) microseconds. The fastest component, $\approx$ 0.5 microsecond, is partly attributed to the unadsorbed dye molecule (i.e., luminescence lifetime of the dye was 0.72 microsecond) [10]; moreover, it is known that the charge recombination is also a multiexponential process which occurs in nanosecond time scale; thus, the ≈0.5-microsecond component could also be due to recombination between Ru(III) and electrons injected into SnO_2. The second microsecond time constant ($\tau_2 = 30.6 \pm 0.5$ (40%) microseconds) reflects the recombination between Ru(III) and the electrons injected into SnO_2; from both time constants, effective average rate constant of $8 \times 10^4\ s^{-1}$ could be calculated. On the other hand, a multiexponential fitting of the 470 nm kinetic for complex (**1**), which contains also a component corresponding to the tyrosine-to-Ru(III) electron transfer, results in three time constants $\tau_1 \approx 0.5$ (60%) microsecond, $\tau_2 = 30.6 \pm 0.5$ (4%) microseconds, and $\tau_3 = 1.3 \pm 0.2$ (36%) microseconds with an effective average rate constant of $5.1 \times 10^5\ s^{-1}$ for tyrosine-to-Ru(III) and recombination between Ru(III) and electrons injected into SnO_2. Moreover, the analysis of the kinetics for complex (**1**) data measured at 410 nm, which corresponds to the formation of the tyrosyl radical, gave the same time constant (within the experimental error) as at 470 nm. On the other hand, in case of complex (**1a**), which has no tyrosine moiety, kinetics measured at 410 nm reflect only the absorption recovery due to the recombination between Ru(III) and SnO_2 electrons and gave the same time constant as at 470 nm.

The rate constant for the intramolecular electron transfer from tyrosine to Ru(III) in the presence of SnO_2 ($k = 5.1 \times 10^5\ s^{-1}$) was faster than the one obtained for the same complex in the presence of TiO_2 ($k = 3.8 \times 10^5\ s^{-1}$) and indeed faster than the rate obtained in the presence of an external electron acceptor MV^{2+} in solution [9]. In fact, analysis of kinetic traces is a little bit complicated and it is not easy to resolve the rate constants of the two steps—the rate constant for the tyrosine-to-Ru(III) and the rate constant for the recombination between Ru(III) and electrons injected into SnO_2 due to the competition between them. On the other hand, even with the competition between the two processes, the average effective rate constants still could be estimated for both processes because the analysis of the kinetics data at 470 nm or 410 nm for complex (**1**) contains component which corresponds to the tyrosine-to-Ru(III) electron transfer, while the kinetics data at the same wavelength for the analogue reference complex (**1a**) reflect only the charge recombination process; moreover, even with the poorly defined kinetic, it is clear that the tyrosyl radical formation is improved by a factor of two compared to the (**1**)-TiO_2 system. From the above results, it seems that using SnO_2 as an electron acceptor increases the efficiency of the attachment of complex (**1**) on the surface of the semiconductor up to unity which slows the back electron recombination, slightly increases the electron transfer rate constant, and indeed improves the efficiency of the tyrosyl radical formation. Moreover, the use of SnO_2 seems to improve the separation of the recombination process from the tyrosine-Ru(III) elec-tron transfer, but still suffers from a competitive back elec-tron recombination which, in fact, is responsible for the rel-atively low yield of the tyrosine-Ru(III) electron transfer.

4. CONCLUSION

We have demonstrated that the anchoring of $Ru(bpy)_3$ complex (**1**) with four carboxylic acid groups linked to the bpy ligands with tin (IV) dioxide, SnO_2, improves the attachment of the dye onto the surface of the semiconductors ($K_a = 2.3 \times 10^6\ M^{-1}$ with a degree of association up to 99%). Anchoring of complex (**1**) to SnO_2 not only enables ultrafast injection of electrons from the excited MLCT state into the conduction band of SnO_2, but also improves the second intramolecular electron transfer from the tyrosine moiety to the photogenerated Ru(III) ($K_{ET} \sim 5 \times 10^5\ s^{-1}$). The second intramolecular electron transfer step (i.e., the rate-limiting step) leads to the formation of tyrosyl radical which can be observed at 410 nm. The yield of Ru(III)-tyrosyl radical conversion is indeed higher (~32%) than the case of TiO_2, but still limited as a result of a competing charge recombination between Ru(III) and the photoinjected electrons in the SnO_2 transfer. We can conclude that using the nanocrystalline SnO_2 slows the charge recombination, thus enhancing the Ru(III)-to-tyrosyl radical conversion, and therefore improves the functionality of the system. It is important to emphasize on the needs for the design of a more efficient complex to overcome the charge recombination problem through increasing the space between the positive charge density of the Ru and the semiconductor, which could slow down the charge recombination and thus enhance the tyrosyl radical formation. Recently, faiz et al. [13] demonstrated that the incorporation of α-cyclodextrin (α-CD) into ruthenium dye improves the power conversion efficiency in solid-state dye sensitized solar cell (i.e., the efficiency of the cell sensitized with Ru-dye incorporated with α-CD is increased by 40% compared to the Ru-dye without α-CD). We think that using a similar idea of incorporating α-CD with our complex (**1**) could improve the functionality of the system through slowing down the charge recombination rate and, therefore, increase the tyrosyl radical formation.

ACKNOWLEDGMENTS

The author would like to thank Professor Villy Sundström for enabling him to use his laboratory facilities to perform all the necessary measurements needed for the accomplishment of this work. Many thanks to University of Al al-Bayt for providing the author with its facilities to conduct this work, and special thanks to Dr. Fatima-Azzahra Delmani for her criticized reading.

REFERENCES

[1] C. W. Hoganson and G. T. Babcock, "A metalloradical mechanism for the generation of oxygen from water in photosynthesis," *Science*, vol. 277, no. 5334, pp. 1953–1956, 1997.

[2] M. Yagi and M. Kaneko, "Molecular catalysts for water oxidation," *Chemical Reviews*, vol. 101, no. 1, pp. 21–36, 2001.

[3] C. Tommos, X.-S. Tang, K. Warncke, et al., "Spin-density distribution, conformation, and hydrogen bonding of the redox-active tyrosine YZ in photosystem II from multiple electron magnetic-resonance spectroscopies: implications for photosynthetic oxygen evolution," *Journal of the American Chemical Society*, vol. 117, no. 41, pp. 10325–10335, 1995.

[4] C. W. Hoganson, N. Lydakis-Simantiris, X.-S. Tang, et al., "A hydrogen-atom abstraction model for the function of YZ in photosynthetic oxygen evolution," *Photosynthesis Research*, vol. 46, no. 1-2, pp. 177–184, 1995.

[5] V. K. Yachandra, V. J. DeRose, M. J. Latimer, I. Mukerji, K. Sauer, and M. P. Klein, "Where plants make oxygen: a structural model for the photosynthetic oxygen-evolving manganese cluster," *Science*, vol. 260, no. 5108, pp. 675–679, 1993.

[6] L. Sun, L. Hammarström, B. Åkermark, and S. Styring, "Towards artificial photosynthesis: ruthenium-manganese chemistry for energy production," *Chemical Society Reviews*, vol. 30, no. 1, pp. 36–49, 2001.

[7] A. Magnuson, H. Berglund, P. Korall, et al., "Mimicking electron transfer reactions in photosystem II: synthesis and photochemical characterization of a ruthenium(II) tris(bipyridyl) complex with a covalently linked tyrosine," *Journal of the American Chemical Society*, vol. 119, no. 44, pp. 10720–10725, 1997.

[8] A. Magnuson, Y. Frapart, M. Abrahamsson, et al., "A biomimetic model system for the water oxidizing triad in photosystem II," *Journal of the American Chemical Society*, vol. 121, no. 1, pp. 89–96, 1999.

[9] M. Sjödin, S. Styring, B. Åkermark, L. Sun, and L. Hammarström, "Proton-coupled electron transfer from tyrosine in a tyrosine-ruthenium- tris-bipyridine complex: comparison withtyrosineZ oxidation in photosystem II," *Journal of the American Chemical Society*, vol. 122, no. 16, pp. 3932–3936, 2000.

[10] R. Ghanem, Y. Xu, J. Pan, et al., "Light-driven tyrosine radical formation in a ruthenium-tyrosine complex attached to nanoparticle TiO2," *Inorganic Chemistry*, vol. 41, no. 24, pp. 6258–6266, 2002.

[11] Y. Tachibana, J. E. Moser, M. Grätzel, D. R. Klug, and J. R. Durrant, "Subpicosecond interfacial charge separation in dye-sensitized nanocrystalline titanium dioxide films," *Journal of Physical Chemistry*, vol. 100, no. 51, pp. 20056–20062, 1996.

[12] T. Hannappel, B. Burfeindt, W. Storck, and F. Willig, "Measurement of ultrafast photoinduced electron transfer from chemically anchored Ru-dye molecules into empty electronic states in a colloidal anatase TiO2 film," *Journal of Physical Chemistry B*, vol. 101, no. 35, pp. 6799–6802, 1997.

[13] Y. Tachibana, S. A. Haque, I. P. Mercer, J. R. Durrant, and D. R. Klug, "Electron injection and recombination in dye sensitized nanocrystalline titanium dioxide films: a comparison of ruthenium bipyridyl and porphyrin sensitizer dyes," *Journal of Physical Chemistry B*, vol. 104, no. 6, pp. 1198–1205, 2000.

[14] J. B. Asbury, R. J. Ellingson, H. N. Ghosh, S. Ferrere, A. J. Nozik, and T. Lian, "Femtosecond IR study of excited-state relaxation and electron-injection dynamics of Ru(dcbpy)2(NCS)2 in solution and on nanocrystalline TiO2 and AI2O3 thin films," *Journal of Physical Chemistry B*, vol. 103, no. 16, pp. 3110–3119, 1999.

[15] C. Bauer, G. Boschloo, E. Mukhtar, and A. Hagfeldt, "Ultrafast studies of electron injection in Ru dye sensitized SnO2 nanocrystalline thin film," *International Journal of Photoenergy*, vol. 4, no. 1, pp. 17–20, 2002.

[16] K. Kalyanasundaram, *Photochemistry of Polypyridine and Porphyrin Complexes*, chapter 6, Academic Press, London, UK, 1992.

[17] T. J. Meyer, "Chemical approaches to artificial photosynthesis," *Accounts of Chemical Research*, vol. 22, no. 5, pp. 163–170, 1989.

[18] J. B. Asbury, E. Hao, Y. Wang, H. N. Ghosh, and T. Lian, "Ultrafast electron transfer dynamics from molecular adsorbates to semiconductor nanocrystalline thin films," *Journal of Physical Chemistry B*, vol. 105, no. 20, pp. 4545–4557, 2001.

[19] R. Argazzi, C. A. Bignozzi, T. A. Heimer, F. N. Castellano, and G. J. Meyer, "Light-induced charge separation across Ru(II)-modified nanocrystalline TiO2 interfaces with phenothiazine donors," *Journal of Physical Chemistry B*, vol. 101, no. 14, pp. 2591–2597, 1997.

[20] Md. K. Nazeeruddin, S. M. Zakeeruddin, R. Humphry-Baker, et al., "Acid-base equilibria of (2,2'-bipyridyl-4,4'-dicarboxylic acid)ruthenium(II) complexes and the effect of protonation on charge-transfer sensitization of nanocrystalline titania," *Inorganic Chemistry*, vol. 38, no. 26, pp. 6298–6305, 1999.

[21] S. Ferrere, A. Zaban, and B. A. Gregg, "Dye sensitization of nanocrystalline tin oxide by perylene derivatives," *Journal of Physical Chemistry B*, vol. 101, no. 23, pp. 4490–4493, 1997.

[22] C. Chen, X. Qi, and B. Zhou, "Photosensitization of colloidal TiO2 with a cyanine dye," *Journal of Photochemistry and Photobiology A*, vol. 109, no. 2, pp. 155–158, 1997.

[23] P. V. Kamat, "Photoelectrochemistry in particulate systems. 9. Photosensitized reduction in a colloidal titania system using anthracene-9-carboxylic acid as the sensitizer," *Journal of Physical Chemistry*, vol. 93, no. 2, pp. 859–864, 1989.

[24] J. Moser and M. Grätzel, "Photosensitized electron injection in colloidal semiconductors," *Journal of the American Chemical Society*, vol. 106, no. 22, pp. 6557–6564, 1984.

[25] A. M. W. Cargill Thompson, M. C. C. Smailes, J. C. Jeffery, and M. D. Ward, "Ruthenium tris-(bipyridyl) complexes with pendant protonatable and deprotonatable moieties: pH sensitivity of electronic spectral and luminescence properties," *Journal of Chemical Society, Dalton Transactions*, no. 5, pp. 737–744, 1997.

[26] M. Hilgendorff and V. Sundström, "Dynamics of electron injection and recombination of dye-sensitized TiO2 particles," *Journal of Physical Chemistry B*, vol. 102, no. 51, pp. 10505–10514, 1998.

[27] J. Desilvestro, D. Dounghong, M. Kleijin, and M. Grätzel, "Tris(2,2'-bipyridine-4,4'-dicarboxylic acid)ruthenium(II), a redox sensitizer affording water oxidation to oxygen in the absence of heterogeneous catalyst," *Chimia*, vol. 39, p. 102, 1985.

[28] M. Sjödin, R. Ghanem, T. Polivka, et al., "Tuning proton coupled electron transfer from tyrosine: a competition between concerted and step-wise mechanisms," *Physical Chemistry Chemical Physics*, vol. 6, no. 20, pp. 4851–4858, 2004.

[29] E. J. Land and W. A. Prütz, "Reaction of azide radicals with amino acids and proteins," *International Journal of Radiation Biology*, vol. 36, no. 1, pp. 75–83, 1979.

[30] J. Faiz, A. I. Philippopoulos, A. G. Kontos, P. Falaras, and Z. Pikramenou, "Functional supramolecular ruthenium cyclodextrin dyes for nanocrystalline solar cells," *Advanced Functional Materials*, vol. 17, no. 1, pp. 54–58, 2007.